Characterization of the propeller for the experimental evaluation of the aerodynamic rotor/propeller interactions in hybrid compound helicopters

Lefevre Lauriane, Vianney Nowinski

TITLE: Characterization of the propeller for the experimental evaluation of the aerodynamic rotor/propeller interactions in hybrid compound helicopters
NAME & First name of main author: LEFEVRE Lauriane
NAME & First name of co-authors: **- NOWINSKI Vianney**
Address (Department/Institute): **ONERA – DAAA/ELV** **5 rue des fortifications, 59000 Lille, France**
E-mail address of main author: lauriane.lefevre@onera.fr
Phone number of main author: +33 3 20 49 69 80
Date of birth of all authors: **- LEFEVRE Lauriane : 11/17/1996** **- NOWINSKI Vianney : 07/18/1988**

Introduction

Helicopters have always been recognized for their vertical take-off and landing (VTOL) and hovering capabilities. While the demand has increased due to the multiplication of air transports, the military and civil needs cannot be reached by the classical configurations because of 1) a limited maximum speed, 2) a low load capacity, 3) a small autonomy, and 4) a questionable comfort due to vibrations and noises … In that context, the compound helicopters have been designed.

Including additional rotors and/or lift wings, those setups entail a rotor slow-down. Different compound configurations have been studied throughout the years: the tilt rotor, the coaxial compound, the tandem helicopter, the simple lift wing… This study focuses on the hybrid compound helicopter, composed of two side propellers mounted on a lift wing as shown in Figure 1. On top of increasing the maximum speed while preserving hovering abilities, the side propellers create an efficient anti-torque facilitating the piloting of the aircraft.

Figure 1 - Eurocopter X3 (left) and Sikorsky RACER (right)

However, compound helicopters are subject to complex interactions, mainly between the different rotating elements. Research has been conducted to study rotor/wing [1]–[5], rotor/fuselage [6]–[8] and wing/propeller interactions [9], but no investigation of the rotor/propeller interactions has been published to date. In this context, this work focuses on the experimental study of the

rotor/propeller interactions, and this paper presents the exhaustive aerodynamic characterization of the propeller.

The experiments took place in the ONERA L2 subsonic wind tunnel with off-the-shelf components. Varying wind speed, rotational speed and side-slip angle, the ideal flight conditions were identified to prepare the characterization of the assembly. The good concordance between numerical and experimental data validated the previous numerical tools.

Experimental setup

Propeller

The first step of this experimental study consists in characterizing the propeller's performances in different flight conditions. Considering the Dauphin 365N model (scale 1/7.7) used for further experiments, the propellers were chosen to mimic the Eurocopter X3 dimensions as shown in Figure 2.

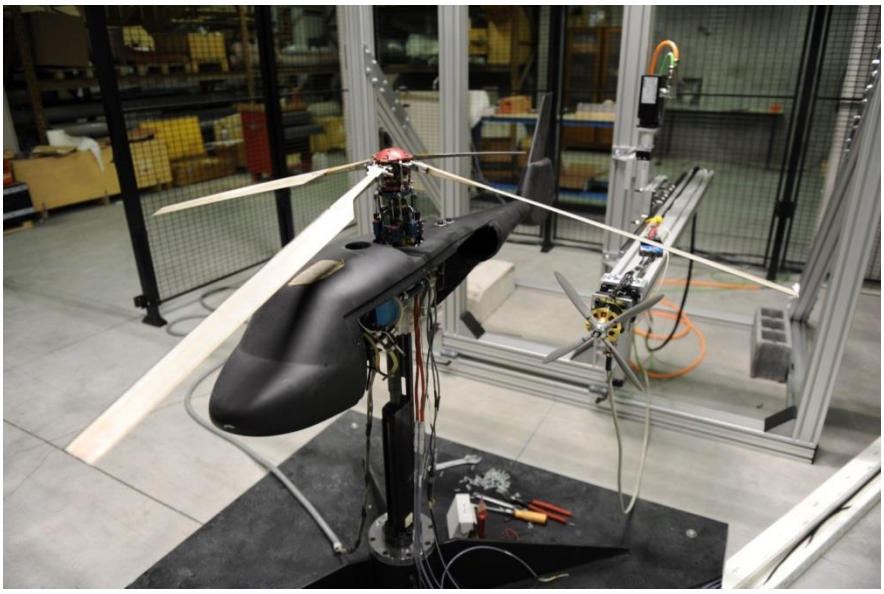

Figure 2 – Installation of the small-scale Dauphin365N and APC11x06-4 propeller

Two 4-blades profiles supplied by APC propeller were considered: 11x09-4 and 11x06-4. To preserve the geometric ratio between the main rotor and the propeller, the propeller has a diameter of 0.28m (11 inches). The only difference between the two profiles is the blade angle (namely 9° and 6°). The blades are made of glass filled nylon. The profiles of the blade were furnished by the supplier, and the polar were obtained using the elsA 2D CFD software for low Reynolds numbers. The coherence of the results was certified using the K-omega model.

To maximize the aerodynamic efficiency of the propeller, a cone has been designed. A fairing has been implemented to isolate the aerodynamic efforts from the flux created by the propeller and by the wind-tunnel. The efficiency of those installations is discussed in this paper.

Measures are performed using the AMTI MC3A 6-axis balance. The characteristics are: non linearity of ± 0.2 % at full scale, transverse sensibility lower than 2%. The balance is equipped with a GEN5 conditioner. The assembly is also equipped with accelerometers and a resistance thermometer (PT100).

For each flight condition, the data is measured for 30 seconds at a frequency of 3000Hz. The measures are acquired with LabVIEW, also used to monitor the evolution of the efforts and to set the rotational speed of the propeller. The post treatment is performed using a house made python code.

Wind tunnel

Experimental studies were conducted in the ONERA large size-low speed L2 wind tunnel. This installation has been in operation since 1968 for naval, industrial and aeronautical applications with a large panel of measurement techniques.

The test-section is 6 meters wide, 2.4 meters high and 13 meters long. To adapt the assembly, a rotating plate of diameter 5.96 meters is integrated into the wind tunnel floor. The measured drift angle is set with an over-estimated uncertainty of 0.1°. The center of the rotating disk is located 6.5 meters downstream of the honey comb.

Downstream of the test section, a small divergence to a width of 2.8 meters is observed to fit the 18 fans divided in 3 horizontal lines and 6 columns. All together, the fans provide a power of 125 kW, allowing the velocity to reach 19 m/s.

The flow is then vented to the rear part of the hall where it freely diffuses to the sides and top before returning to the entrance of the tunnel with a slow velocity.

The wind tunnel operates at ambient atmospheric conditions. The humidity, the ambient static pressure and temperature are measured in the undisturbed air in the hall to evaluate the influence of the atmospheric conditions on the air density. No cooling devices are used to keep the flow at a constant low temperature but, considering the low velocities involved, the natural heat conduction only generates a 5°C per hour temperature increase in continuous operations. The flow passage ensures the cooling of the electric engines of the fans.

The turbulence profile shows values up to 7.6% close to the walls, but les than 0.5% in the middle of the section. Those values depend on the wind speed, and on the geometry of the profile. Considering the small dimensions of the propeller, the wall and blockage effects are assumed negligible. This hypothesis is verified when studying the effect of the side-slip angle on the performances.

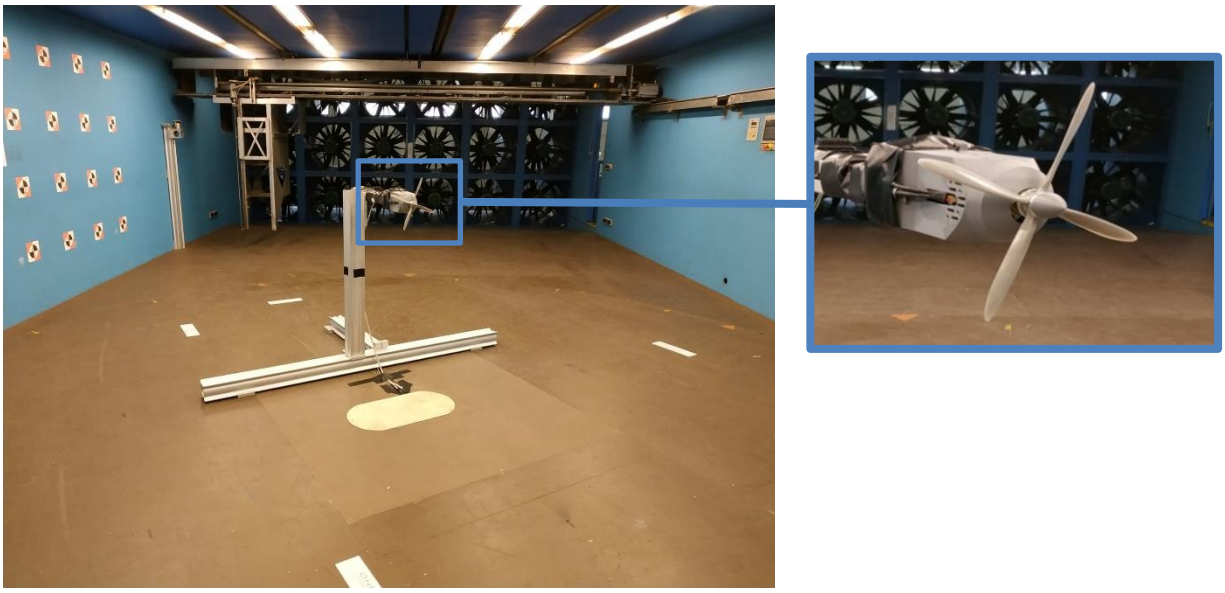

Figure 3 - Small scale propeller mounted in the L2 subsonic wind tunnel

Computational models

Unsteady free wake approach

The first numerical approach used during this study was PUMA (Potential Unsteady Methods for Aerodynamics), a free wake code developed at ONERA. Particularly used in the pre-design phases for fixed and rotating wings, the code is based on a coupling between the kinematic and the free aerodynamic modules.

A rigid body system is used to determine the kinematic module. The structure is composed of links and articulations, and the hypothesis of a negligible deformation regardless of the external constraints is made to simplify the computation.

The aerodynamic module is determined using a free wake model and a lifting line approach. The free wake model describes the unsteady evolution of the wake modelled by a potential discontinuity surface, based on the Mudry theory [10]. The potential approach can be used to consider any surface in the wake. The lifting line theory predicts the lift distribution over a three-dimensional wing based on its 2D polars. Based on the simplification of the wing into a simple line at the quarter of the chord, this approach considers the 3D corrections for blade sweep. Therefore, this theory is particularly adapted for tapered wings, which is the case for the considered propeller.

The wing is divided into sections whose dimensions depend on the local angle of the physical wing. Based on the Kutta-Joukowski theorem, the concept of circulation is introduced to reflect the influence of the neighboring sections [11]. The lift and the drag coefficient can be determined by integrating the circulation terms over the section.

To balance between accuracy and resource mobilization, different temporal discretizations are available. OpenMP is used to reduce the computational time. The Multilevel Fast Multiple Method is set to speed up the resolution of the equations of the velocities induced by the wake of each section.

The computation parameters were based on previous studies. Depending on the case, the last 3 to 5 wake revolutions were averaged and 8 to 15 revolutions were computed. While most of the cases reached the convergence with those parameters, for low advance ratio or for specific side-slip angles unsteadiness was important. Some numerical parameters had to be modified to stabilize the computation, which might have affected the obtained results.

The free wake approach presents several limitations: 1) only incompressible, non viscous and steady flows can be considered and 2) the theory cannot be applied for swept wings, or for low aspect ratio wings. Considering the very low speeds involved and the geometry of the blades, the up-listed limitations do not interfere with our case. In that context, further studies including a CFD code were conducted to validate the model. In all the numerical studies, the fuselage of the helicopter was not considered. This study will evaluate the coherence of the numerical results and propose, if applicable, corrections to the numerical tools.

ElsA

ElsA is a URANS CFD solver developed at ONERA since 1997. Suitable for various configurations, going from the full plane to the helicopter and the compressor, the software can consider the aeroelastic effects.

The grids of the rotor and of the propeller blades are built using Pointwise®. The background mesh is a Cartesian grid based on an Octree approach, counting 9 levels with a ½ scale between each level. The computational parameters were set using the experience of the previous studies. The convergence is obtained when the variation of mean thrust between two revolutions remains low, which is easily reachable in a few revolutions.

In this study, elsA was used to determine the airfoil data needed in the PUMA computation, considering a constant Re/Mach ratio (with Re the Reynolds number) corresponding to the studied propeller. The CFD software was also consulted for more complete computations to validate the PUMA approach and to determine more precisely the interactional rotor/propeller effects.

Results

Preliminary studies

The first step of this study consisted in understanding the critical flight conditions. To do so, the model of the DAUPHIN 365N was implemented in the elsA code to examine the influence of the main rotor's wake on the propeller, and the propeller's wake [12].

For hovering flights, the rotor wake generates a 10m/s 90° incidence flow on the propeller. At high advance ratios, the rotor wake passes over the propeller and the flux is sucked. This generates a decrease of the propeller inflow velocity which increases the local angle of attack, and ultimately increases the thrust. In the case where the isolated propeller operated at its maximal thrust capacity, the interactions lead to a flux separation and a drastic loss of aerodynamic efficiency. The emergence of radial components of the propeller's inflow velocity, as well as the increase of the pitching moment can also be highlighted. Depending on the positioning of the propeller, the interactions may severely impact the maneuverability of the helicopter.

On the other hand, the influence of the propeller on the rotor is low. An increase of power of about 3% arises at high advance ratio. The hypothesis of a rotor/propeller decoupling at high advance ratio is done for further study. This hypothesis will be verified when comparing the data of the isolated characterizations with the performances of the full model.

Experimental results

Tests were conducted considering different parameters:

- The wind speed varies from 0m/s to 19m/s, thus operating through all the L2 capabilities. To suppress the inertial effects, a stabilization time is observed at each wind speed change.
- The rotational speed of the propeller varies from 0rpm to 9,500rpm. The rotational speed is set with an uncertainty of ±30 rpm. This study aims to extract trend curves to determine the ideal functioning modes.
- The side-slip angle varies from -30° to +90°. The symmetry of the efforts, as well as the influence of the isolated rotor wake are studied.
- Two propellers profiles are tested to determine the influence of the blade angle on the performances.
- The influences of the fairing and of the cone are discussed.

All the figures below show the 95% confidence interval in red.

As shown in Figure 4, the effective traction (Fx) of the propeller is increased when the rotational speed is increased or when the wind speed is decreased. Unlike what was expected, the plane forces (horizontally Fy and vertically Fz) and moments are not null. This is caused by multiple sources: 1) an unbalanced assembly, 2) a non-symmetrical wind due to an imprecise adjustment of the rotating plate, and 3) the asymmetric intrusive measurement bench blocking the development of the propeller's wake. The influence of those parameters is maximal at low speeds.

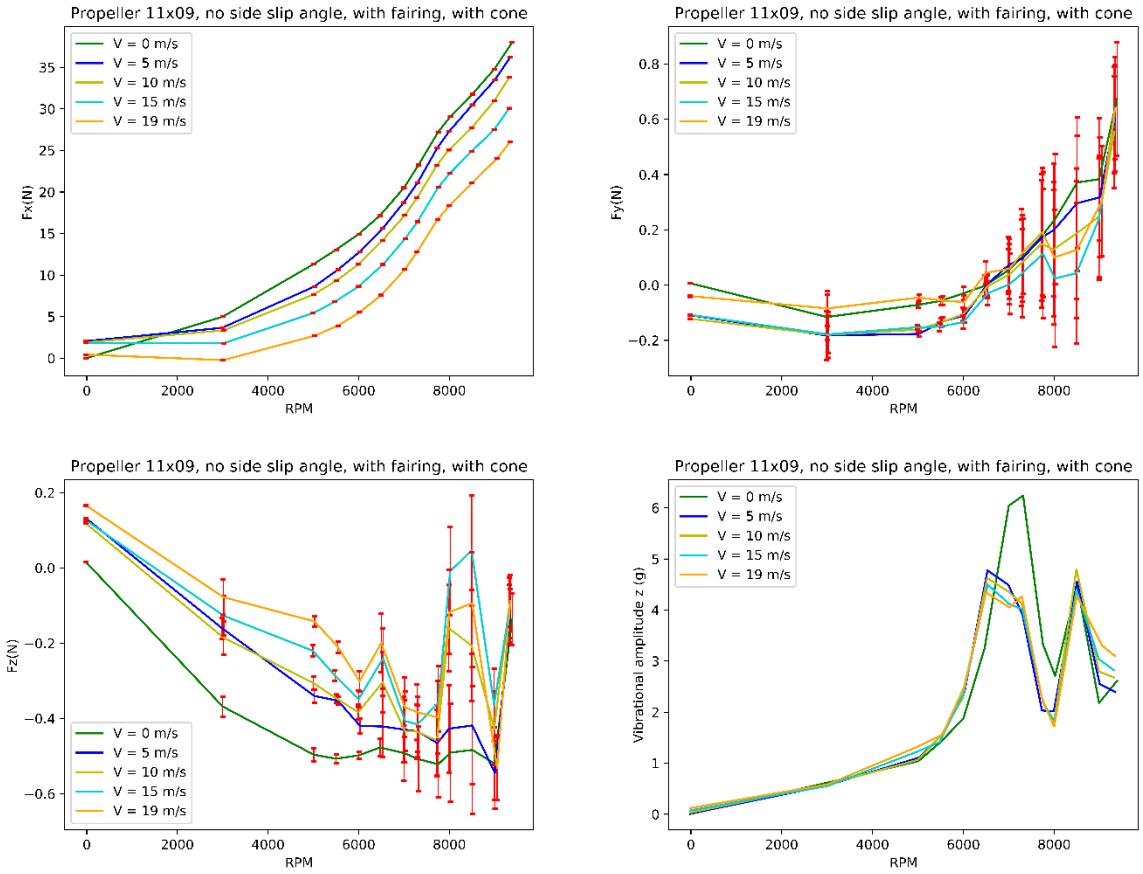

Figure 4 - Mean efforts and vibrations depending on the propeller rotational speed for different wind speeds

Local maximums and minimums can be observed. Those peaks were coupled with vibrations maximums, thus privileging the hypothesis of resonance of the assembly. A fast Fourier transform highlighted the main resonance frequencies. A 6th order low pass filtering has been applied at 150Hz to limit the standard deviation of the measures, but the same profile was conserved. A study with the isolated measurement bench showed that the resonance peaks appears even when the propeller is not implanted. The hypothesis that the vibrations are mainly caused by the eigenmode of the structure is privileged.

A fairing and a cone have been installed (Figure 5). The fairing decouples the measured forces from the efforts induced by the propeller's wake by isolating the motor and the balance. Examining the results with and without fairing proves that the lateral efforts are mainly caused by the asymmetry of the measurement bench. On top of ensuring the correction of the measures, adding a fairing thus increases the balance of the device. The vibrations are also limited probably due to the stiffening of the device and to the transmission of the wake induced forces behind the balance.

Adding a cone to the tip of the propeller's shaft increases the traction, especially for high rotational speeds in presence of wind. This is explained by a better penetration of the flux resulting from the deletion of the non linearity. Blade root acceleration is also assumed in presence of the cone. Besides, the stability of the structure is maximized by limiting the lateral efforts and the resonance effects.

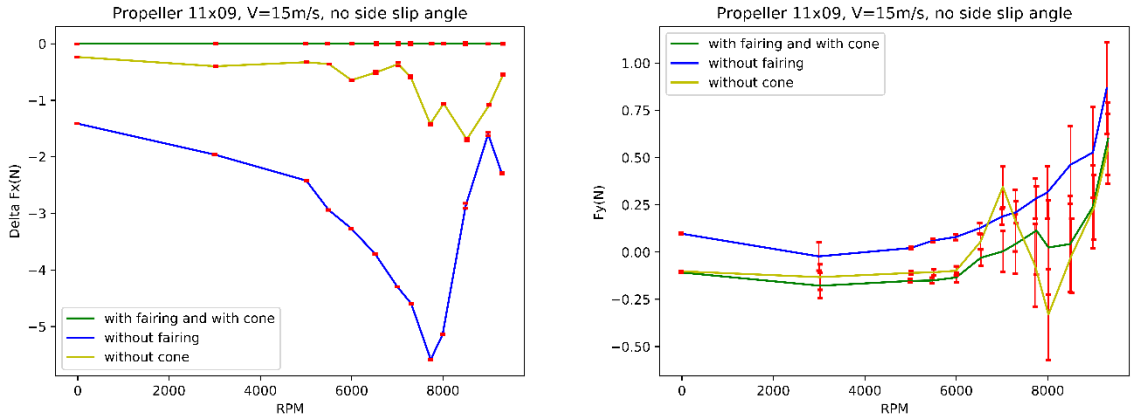

Figure 5 - Mean efforts depending on the propeller rotational speed for different implantations

The side-slip angle influences the performances of the propeller (Figure 6): while the traction remains unchanged in the wind-free case thus proving the absence of wall effects, increasing the angle increases the traction in the presence of wind. The maximal traction is reached for a 90° angle, representing the pure influence of the rotor wake. The plane efforts and the vibrational effects are also increased with the side-slip angle, due to the effects of the wind on the structure and to the strong interactions between the propeller and its wake.

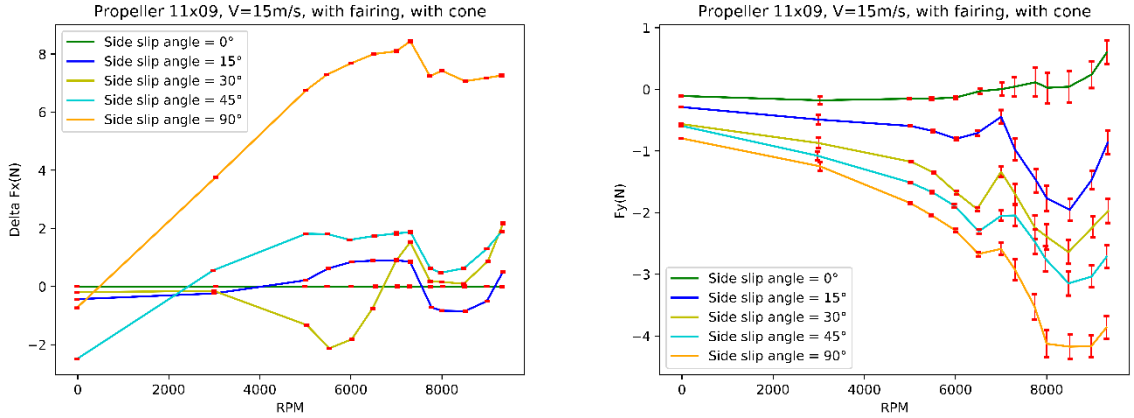

Figure 6 - Mean forces depending on the propeller rotational speed for different side-slip angles

The compound helicopter entails two propellers. Whereas the traction is provided equally by both propellers in forward flight, the anti-torque function is fully ensured by the left propeller. The maximum power is needed to balance the helicopter in hovering flights, which generates an increased wear of the left propeller. To further examine the efforts on both propellers, a symmetry study has been conducted with side-slip angles of 0°, +30° and -30° (Figure 7). Except for measurement errors, the symmetry of the performances is verified.

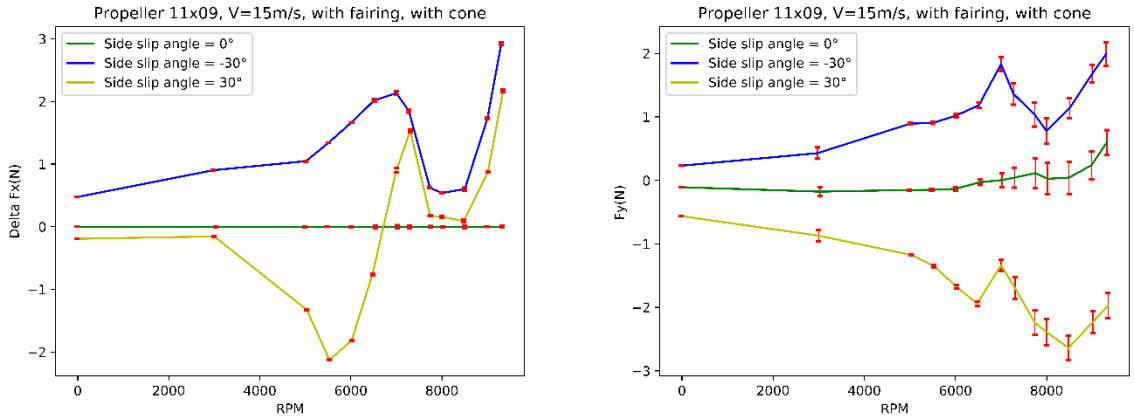

Figure 7 - Mean forces depending on the propeller rotational speed for symmetric side-slip angles

The comparison of the experimental results with the numerical simulations (Figure 8) showed an under estimation of 10% to 15% of the forces by Puma for high rotational speeds. The introduction of side-slip angles enhances that error. Considering the calculus hypothesis and not accounting for the measurement bench in the numerical methods, this error is considered acceptable.

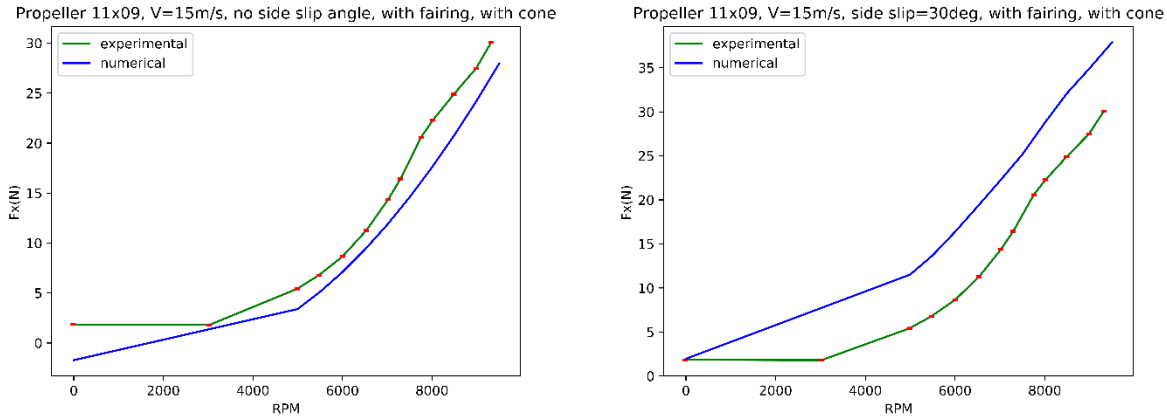

Figure 8 - Experimental and numerical mean traction depending on the propeller rotational speed

Finally, the performances of two propellers were compared (Figure 9). The APC11x09-4 profile generates more traction and less plane efforts. The APC11x06-4 propeller entails less vibration, especially at low rotational speed due to the limited wake. However, a minimal traction is required to ensure the propulsion and the anti-torque functions. For that reason, the 11x09 propeller will be used for further experiments.

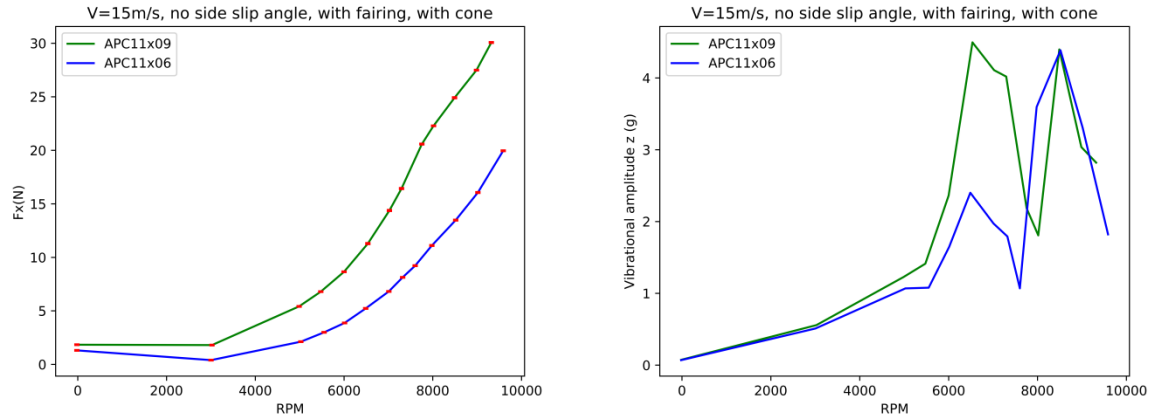

Figure 9 - Mean forces depending on the propeller rotational speed for different propellers

Remarks and discussion

An important divergence caused by the heating of the balance emerged. To limit the conduction, a laminated wooden plate has been installed between the motor and the balance. A linear temperature correction has also been applied. The coefficients were determined experimentally by heating the balance and monitoring the evolutions of the forces and moments. The operation has been repeated five times in different conditions, and the average result was used to correct the efforts. The determined coefficients showed that the moments are not highly impacted by the temperature variation.

Increasing the wind speed lowered the minimal reachable rotation speed with the available device, showing that the wind facilitates the propeller rotation at low speeds. It has also been noticed that a range of rotational speed around the theoretical nominal point (7730rpm) was not reachable. To limit the uncertainties, measures were performed at the limits of the range for all flight conditions.

Tests without wind showed that from 5000rpm, the propeller's wake beget the rotation of the wind tunnel's fan located 6m downstream. At 8000rpm, 6 of the 18 fans were rotating. This characteristic showed that the wake deviates to the left due to the asymmetry of the measurement bench. The design of the full scale propeller is not impacted by that characteristic: the rotational sense of the propellers is determined to benefit from the tip vortices to increase the aerodynamic efficiency.

The repeatability of the measures has been examined for different flight conditions. Stationary tests (V=0m/s and RPM=0rpm) showed an important divergence between the initial measures and the repeated ones, greatly limited by the applied temperature correction. However, the remaining error could not be completely suppressed nor directly linked to external parameters. The measures done at nominal rotational speed with no wind showed a good concordance between the initial and the repeated measures, sparsely impacted by the temperature correction.

A study of the preheating of the measuring tools has been conducted, showing that the cold balance overestimates the forces and underestimates the moments. Around the nominal rotational speed, the lateral efforts also undergo a peak that was not observed with the correctly heated balance. For all the presented results, a pre-heating period has been observed.

The influence of the atmospheric conditions on the environment has been monitored. An increase of temperature coupled with a decrease of pressure and of relative humidity emerged during tests, caused by the influence of the sun on the shed and by the heat generated by the fans of the wind-tunnel. Those fluctuations entailed a typical density variation of 2% during a 2 hours long test, which slightly modifies the speed around the model. No correction has been made to balance those variations.

The validity of the hypothesis used in Puma is also discussed. Considering the maximum rotational speed of 9500rpm for a diameter of 28cm, the tip speed reaches Mach 0.41. Knowing that a flow is supposed incompressible for Mach$\leq$0.3, the compressibility hypothesis is questionable. The non-viscosity and stability hypothesis are verified considering the low speeds involved.

The free wake approach is based on the condition that the propeller's polar are linear, which is verified for local attacks angles between -10° and +20°. However, some cases with specific side-slip angles showed local angle of attack up to 90° due to divergences. In those particular cases the numerical tools were not sufficient to determine the performances of the propeller, proving the importance to couple numerical and experimental data.

Conclusion

The study with no side-slip angle showed that the optimal point is at 8000rpm for high speed winds considering the measurement uncertainties. When introducing side-slip angle, the optimal point is at 7200rpm with the minimal angle. Those points will be used to start the characterization of the full device including the helicopter and the propeller. Considering that the design of the propeller is different than the one implanted on the full scale model, and that the lateral efforts mainly depend on the positioning of the propeller on the full device, this study will not be used directly to design the full scale helicopter.

The case at 90° is particularly interesting because it represents the pure influence of the rotor wake on the propeller. In that situation, the efforts are maximal, which entails an efficient anti-torque and propulsion but generates an anticipated wear of the device. Stall effects can also appear more rapidly. Despite the asymmetry of the bench and the measurement uncertainty, the symmetry of the efforts has also been proven.

This first study highlighted the importance of the fairing to improve the exactness of the measures. The cone slightly increases the aerodynamic efficiency of the propeller. Both devices limit the plane efforts for all the flight conditions.

A good concordance between the experimental and the numerical result has been found. To limit the divergence between the two approaches, the blade has been scanned to implement the real geometry in Puma. No correction has been made to consider the measuring bench, the fairing or the cone in the numerical tools.

The presented results are discussable under three conditions:

1) The temperature correction coefficients were determined experimentally. Their precision is not guaranteed. To limit the divergence sources, the thermal characterization tests were conducted multiple times in different conditions (artificial and natural heating, day and night, heating and cooling, high and low atmospheric pressure …). While the measurement errors are limited, the correction does not entirely correct them.
2) Important standard deviations were observed during the tests, especially for the plane efforts. To limit the uncertainty of the results, each point was measured during 30 seconds at a frequency of 3000Hz.
3) The atmospheric conditions variations slightly modify the density of the air, and consequently the wind speed. Considering the low speeds investigated, no correction has been set.

Acknowledgement

The authors gratefully acknowledge the financial support given by ONERA and the region Hauts-de-France. The technical support of Ronan Boisard for the numerical part and of Jérôme Delva for the experimental setup, and the time and attention given by Antoine Dazin are also thanked

Bibliography

[1] M. Orchard and S. Newman, “The fundamental configuration and design of the compound helicopter,” *J. Aerosp. Eng.*, vol. 217, no. 6, pp. 297–315, Jun. 2003, doi: 10.1243/095441003772538570.

[2] M. Floros and W. Johnson, “Performance Analysis of the Slowed- Rotor Compound Helicopte...: Ingenta Connect,” *J. Am. Helicopter Soc.*, vol. 54, no. 2, p. 22002, Apr. 2009, doi: 10.4050/JAHS.54.022002.

[3] S. Sugawara and Y. Tanabe, “A Study of Rotor/Wing Aerodynamic Interaction at High Speed Flight on a Compound Helicopter,” presented at the 6th Asian/Austrailian Rotorcraft Forum, Heli, Japan, Nov. 2017.
[4] H. Sugawara and Y. Tanabe, “Numerical Investigation of Rotor/Wing Aerodynamic Interactions at High Advance Ratios,” *J. Aircr.*, vol. 0, no. 0, pp. 1–14, doi: 10.2514/1.C035370.
[5] M. Bühler and S. J. Newman, “The aerodynamics of the compound helicopter configuration,” *Aeronaut. J.*, vol. 100, no. 994, pp. 111–120, Apr. 1996, doi: 10.1017/S0001924000027391.
[6] Le Pape A., Gatard J., and Monnier J.-C., “Experimental Investigation of Rotor-Fuselage Aerodynamic Interactions,” *J. Am. Helicopter Soc.*, vol. 52, no. 2, p. 99, Apr. 2007, doi: 10.4050/JAHS.52.99.
[7] T. Renaud, C. Benoît, J.-C. Boniface, and P. Gardarein, “Navier-Stokes computations of a complete helicopter configuration accounting for main and tail rotors effects,” Friedrichshaffen (Germany), Sep. 2003, p. 10.
[8] T. Renaud, M. Smith, M. Potsdam, and D. O’Brien, “Evaluation of isolated fuselage and rotor-fuselage interaction using Computational Fluid Dynamics,” *J. Am. Helicopter Soc.*, vol. 53, no. 1, pp. 3–17, Jan. 2008, doi: 10.4050/JAHS.53.3.
[9] D. P. Witkowski, A. K. H. Lee, and J. P. Sullivan, “Aerodynamic interaction between propellers and wings,” *J. Aircr.*, vol. 26, no. 9, pp. 829–836, Sep. 1989, doi: 10.2514/3.45848.
[10] M. Mudry, “La théorie générale des nappes et filaments tourbillonaires et ses applications à l’aérodynamique instationnaire,” [s.n.], S.l., 1982.
[11] Brian J. Cantwell, *Applied aerodynamics*, vol. 11–13, 14 vols. Stanford, California, 2014.
[12] R. Boisard, “Aerodynamic investigation of rotor/propeller interactions on a fast rotorcraft,” Delft, The Netherlands, Sep. 2018, vol. 13, p. 14.